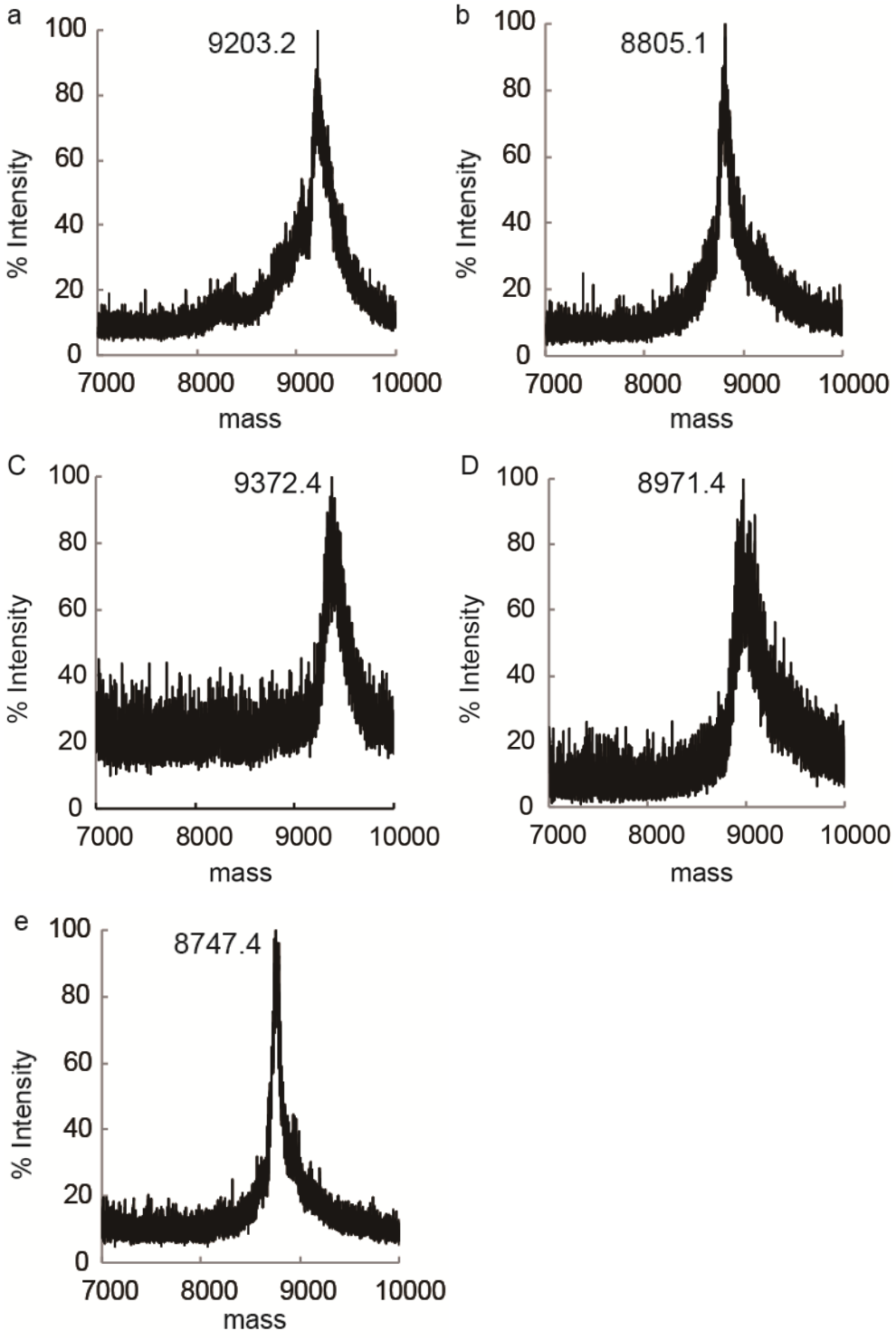

Supplementary Figure 1. Representative MALDI-TOF spectra.

(**a**) c(RGDfK(PEG-PEG))-ligand strand-Cy5, (**b**) Gly-Arg-Gly-Asp-Ser-ligand strand-Cy5, (**c**) c(RGDfK(PEG-PEG))-ligand strand-Cy3B, (**d**) Gly-Arg-Gly-Asp-Ser-ligand strand-Cy3B, and (**e**) QSY 21 labeled anchor oligonucleotide strand.

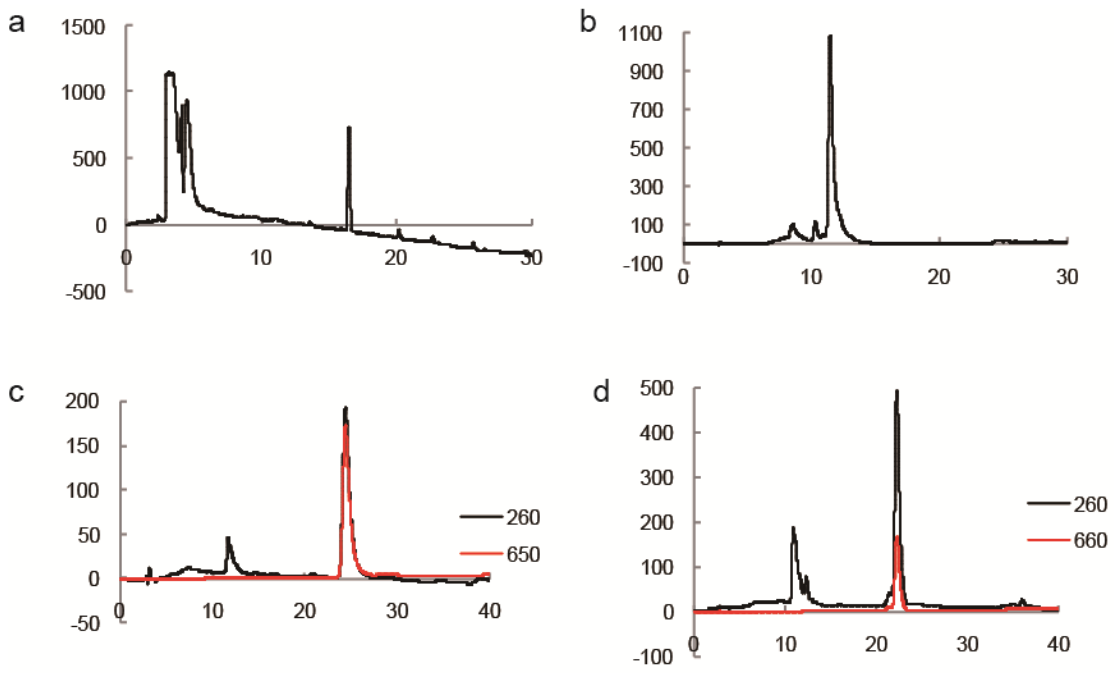

Supplementary Figure 2. Representative HPLC traces of reactions used to generate oligonucleotide conjugates. (**a**) product **1** (structure shown in Supplementary Note 1), (**b**) product **2** (structure shown in Supplementary Note 1), and (**c**) product **3** (structure shown in Supplementary Note 1). HPLC trace in **d** is representative of the products of the QSY 21 anchor oligonucleotide coupling reaction.

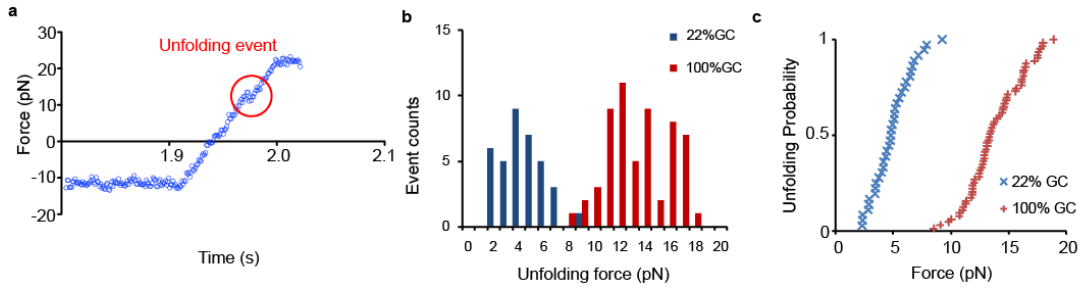

Supplementary Figure 3. 22% and 100% GC content hairpin probe calibration by BFP. (**a**) Example of an unfolding event measured by pulling of a 100% GC content hairpin probe. **(b**) Histogram of unfolding events for the two DNA-based probes that were tested (*n* = 99 hairpins tested). Each event corresponds to the denaturation of a single DNA hairpin probe. (**c**) Cumulative histograms for the 22% and 100% GC content hairpin tension sensor unfolding probability.

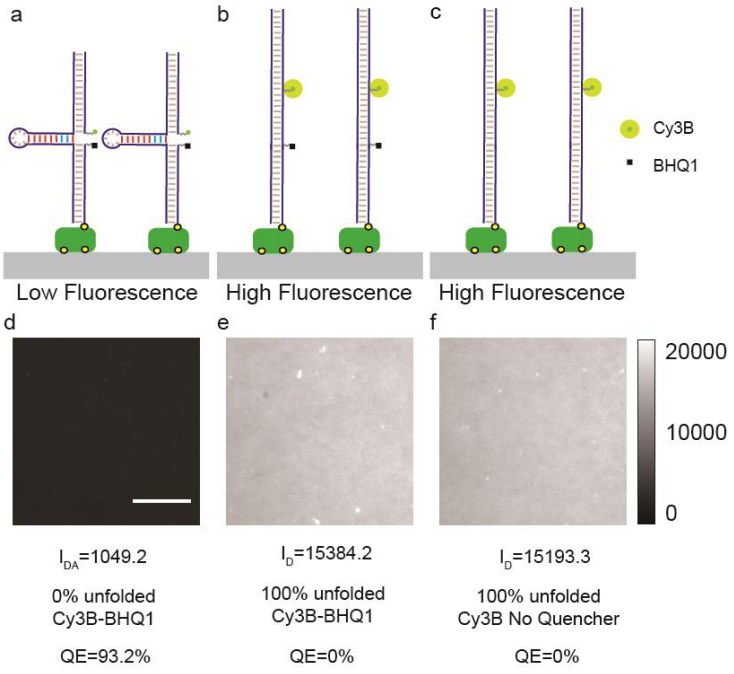

Supplementary Figure 4. Determination of dye quenching efficiency as a function of hairpin folding. To show that the dye is completely dequenched when the hairpin is unfolded, we compared the fluorescence intensity of the probe with and without the quencher. (**a, d**) Representative fluorescence image of a probe surface with the folded (closed) hairpin tagged using the Cy3B-BHQ1 fluorophore-quencher pair. The quenching efficiency (QE) of this sample was ~93%. (**b, e**) Representative fluorescence image of an opened (or unfolded) tension probe surface where the Cy3B and BHQ1 fluorophore and quencher pair was separated by hybridization with a complementary strand to the hairpin region. (**c, f**) Representative fluorescence image of a substrate modified with a probe similar to the one used in (**b**) but lacking the quencher. By comparing the fluorescence intensity of (**b**) and (**c**) we note little difference between samples, indicating that Cy3B is fully dequenched when the hairpin is fully opened. Note that a mechanically-denatured ssDNA hairpin is likely to be extended a greater distance than the duplex probe distance. Therefore, force-induced opening of the tension probes will likely lead to full recovery of the fluorophore intensity.

a

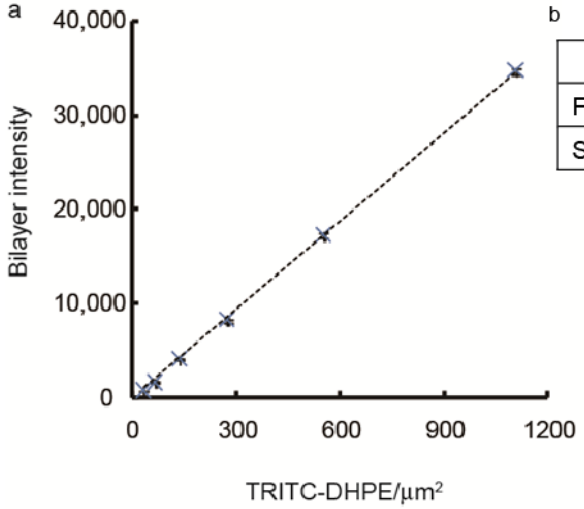

b

	Cy3B 22%GC sensor
F Factor	1.62 ± 0.13
Sensors/ μm^2	419 ± 31

Supplementary Figure 5. Calibration curve for converting fluorescence intensity to molecular density. (**a**) Plot shows a calibration curve relating the fluorescence intensity of TRITC-DHPE – doped supported lipid membranes to their molecular density. (**b**) Table showing the F factor value, which relates the brightness of Cy3B 22% GC tension probes to that of TRITC-DHPE using a fluorescence microscope. By using the calibration curve in (**a**) and the F factor, we determined that the molecular density of Cy3B 22% GC tension probes was 419 $\pm$ 31 sensors/μm^2. This error represents the standard deviation in molecular density across three different substrates.

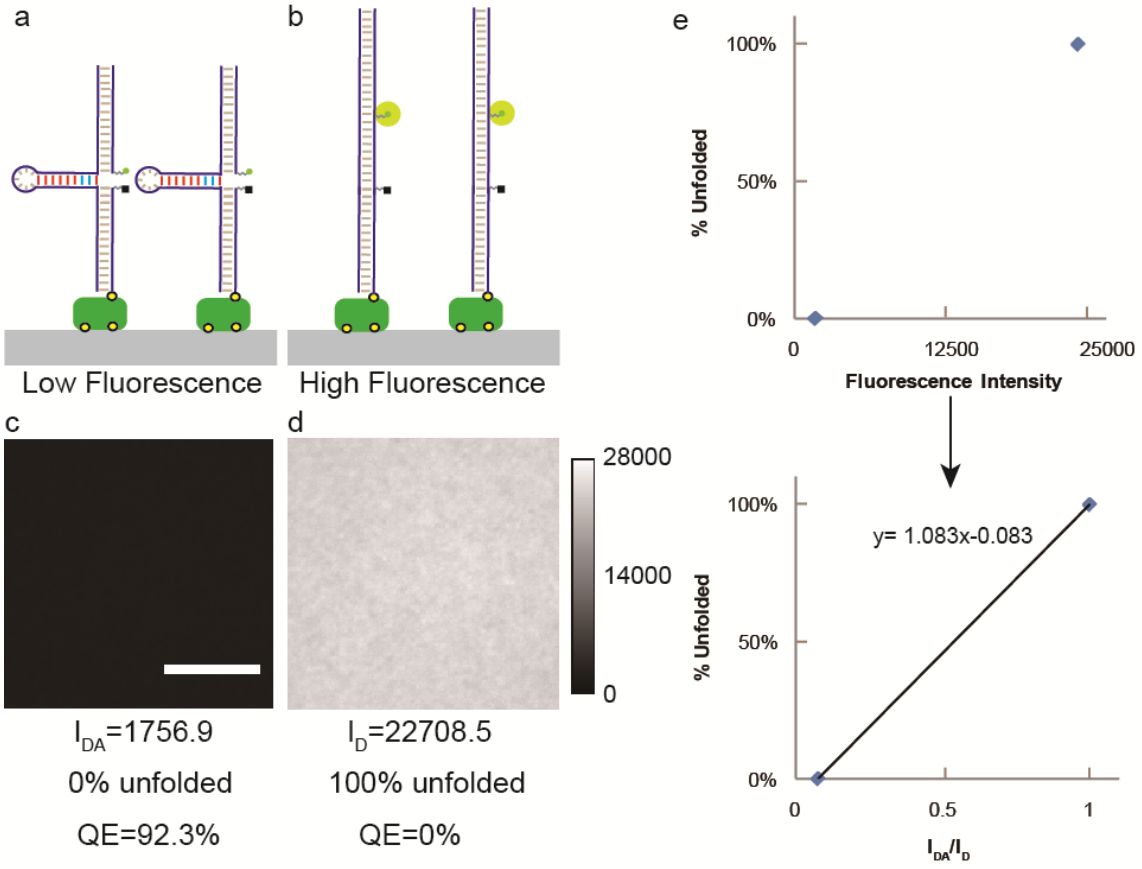

Supplementary Figure 6. Representative example showing how QE (1- I_{DA}/I_D) and % unfolded were determined for tension probes immobilized onto glass substrates. (**a, b**) Schemes showing closed and open MTFM tension probe surfaces. (**c, d**) Representative fluorescence images and quantitative intensity scale bar for the probes shown in (**a**) and (**b**). Scale bar is 10 μm. The corresponding unfolding percentage and QE values for each image are indicated below. Data was obtained using the Cy3B channel in a multiplexed tension probes experiment displaying different values of $F_{1/2}$. (**e**) The conversion function was calculated from the data acquired from **c** and **d**: % unfolded = $(1.083 \times I_{DA}/I_D - 0.083) \times 100$.

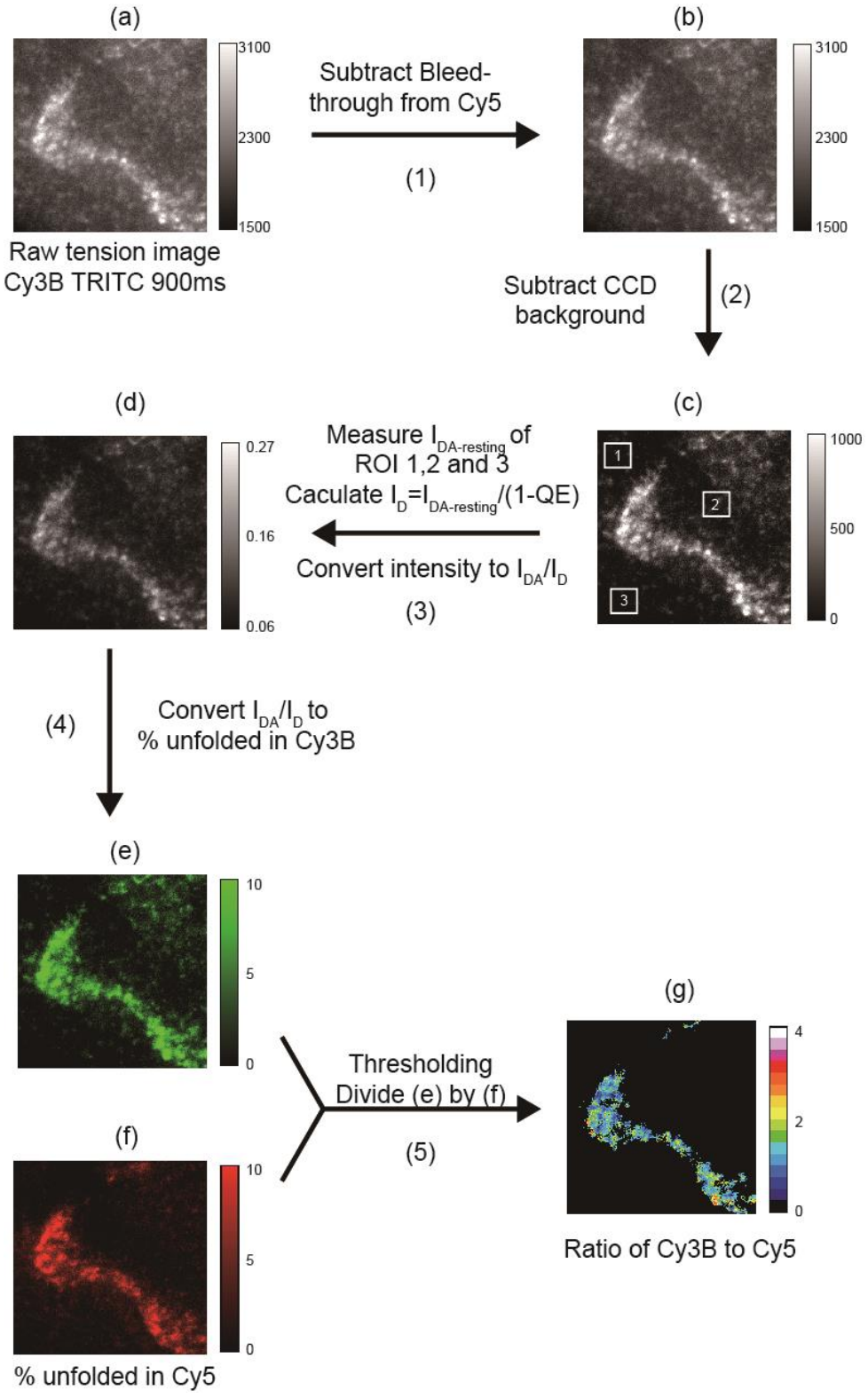

Supplementary Figure 7. **Flow chart describing the steps to convert fluorescence intensity to % unfolded.** See detailed steps in following section. Scale bar 10 μm.

Fluorescence images were converted to “unfolding percent” images by using the following steps (Supplementary Fig. 7):

1) Collect raw fluorescence images of from cells cultured on MTFM DNA-based probes using indicated imaging parameters (see Imaging Parameters section below) (Supplementary Fig. 7a).
2) For multiplexed sensors, subtract bleed-through from other dyes yielding Supplementary Fig. 7b. A bleed-through coefficient was determined by imaging one fluorescent probe (Cy3B, for example) using the alternate filter cube set (Cy5, for example). The bleed-through coefficients are listed in the Imaging Parameters section below.
3) Subtract EMCCD instrumental background from Supplementary Fig. 7b to obtain Supplementary Fig. 7c.
4) Determine the fluorescent intensity of the folded hairpin at resting ($I_{DA\text{-}resting}$) by averaging three regions of interest (box 1, 2 and 3 within Supplementary Fig. 7c). Then, divide $I_{DA\text{-}resting}$ by (1- QE), thus yielding the fluorescence intensity of fully de-quenched surface (I_D). Subsequently, divide the fluorescence intensity (Supplementary Fig. 7c) by I_D, thus yielding an image with values of I_{DA}/I_D, which is the de-quenching efficiency (Supplementary Fig. 7d).
5) Convert I_{DA}/I_D image (Supplementary Fig. 7d) to % unfolded by applying predefined conversion function (see Methods Imaging Parameter and Supplementary Tables 5-9).
6) Repeat the steps outlined above for other fluorescence channels in multiplexed probe experiments. Then, threshold the two images and divide to obtain the ratio of unfolded probes in each channel. Typically, the % unfolded from larger magnitude $F_{1/2}$ probes was divided by the % unfolded image from probes with lower values of $F_{1/2}$.

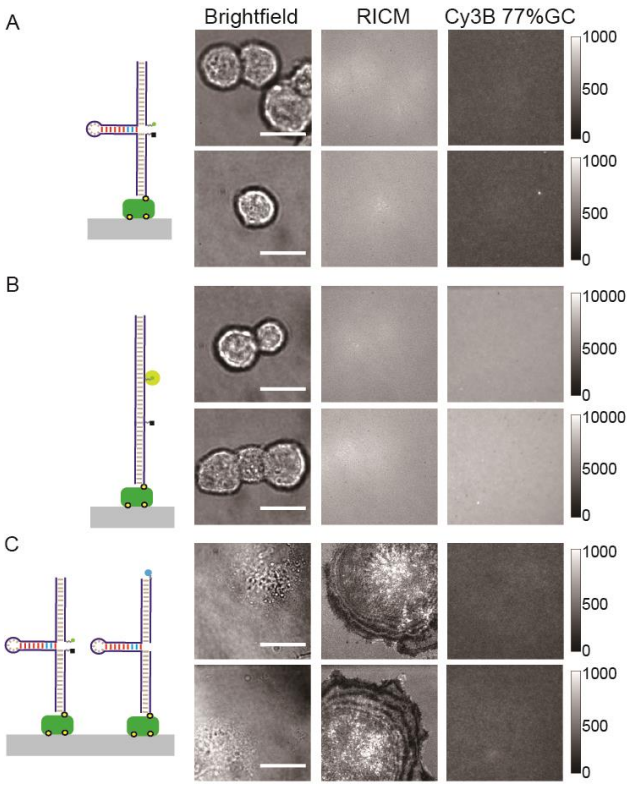

Supplementary Figure 8. Control experiments showing that tension signal is specific to RGD-integrin interactions. (**a**) Representative brightfield, RICM, and fluorescence images of cells plated on quenched sensors lacking adhesive RGD peptides for 30 min. No RICM signal or increase in fluorescence signal was observed for all cells imaged. (**b**) Representative brightfield, RICM, and fluorescence images of cells plated on sensors opened by their complementary strands and lacking the RGD peptides. No cell attachment or fluorescence response was observed after 30 minutes of cell incubation. (**c**) Representative brightfield, RICM, and fluorescence images of cells incubated on a binary mixture of probes, one lacking the RGD peptide, and the second lacking the fluorophore-quencher reporter pair. Cells adhered and spread in this case, but no fluorescence signal was observed after 30 min of cell seeding. Scale bar is 20 μm.

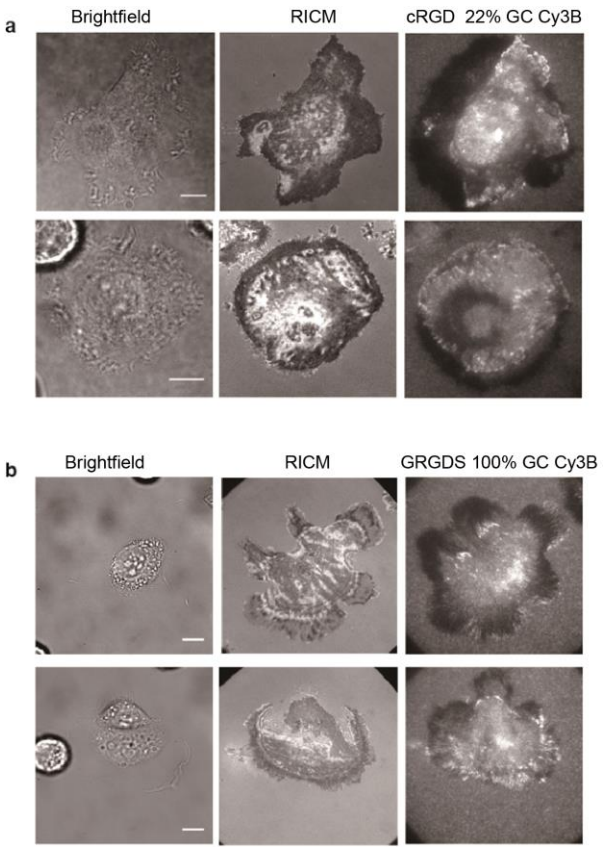

Supplementary Figure 9. Loss of fluorescence signal due to prolonged cell incubation. **(a)** Representative brightfield, RICM, and fluorescence microscopy images of cells incubated on 22% GC tension probes displaying cyclic RGD peptide for 1 hour. **(b)** Representative brightfield, RICM, and fluorescence microscopy images of cells incubated on 100% GC tension probes displaying linear GRGDS peptide for 1 hour. Fluorescence intensity values that are below that of the closed probe appeared under specific regions near the cell, and typically corresponded to cell migration history. Scale bar is 10 μm.

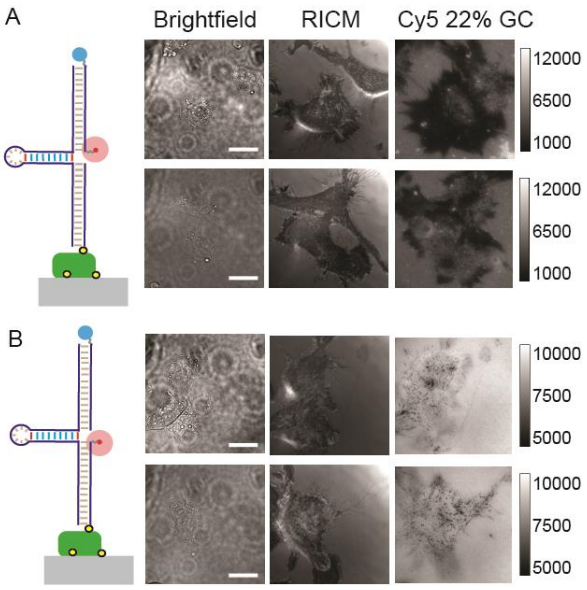

Supplementary Figure 10. Determining the cause of fluorescence signal loss after prolonged cell incubation. (**a**) Control tension probes were synthesized with Cy5 fluorophore coupled to the ligand strand of the sensor, while the anchor strand lacked the quencher. Representative brightfield, RICM, and fluorescence images indicate significant loss of fluorescence signal under cells that were incubated for ~ 1 hr. This suggests dissociation of the upper strand containing the dye. (**b**) Control tension probes were synthesized with Cy5 fluorophore conjugated to the anchor strand of sensor lacking a quencher. Representative brightfield, RICM, and fluorescence images indicate slight loss of fluorescence within punctate regions under cells incubated for ~ 1 hr. This suggests that the anchor strand generally remains in tact at this time point. We speculate that this loss of fluorescence intensity is due to cell-generated nucleases. Scale bar is 20 μm.

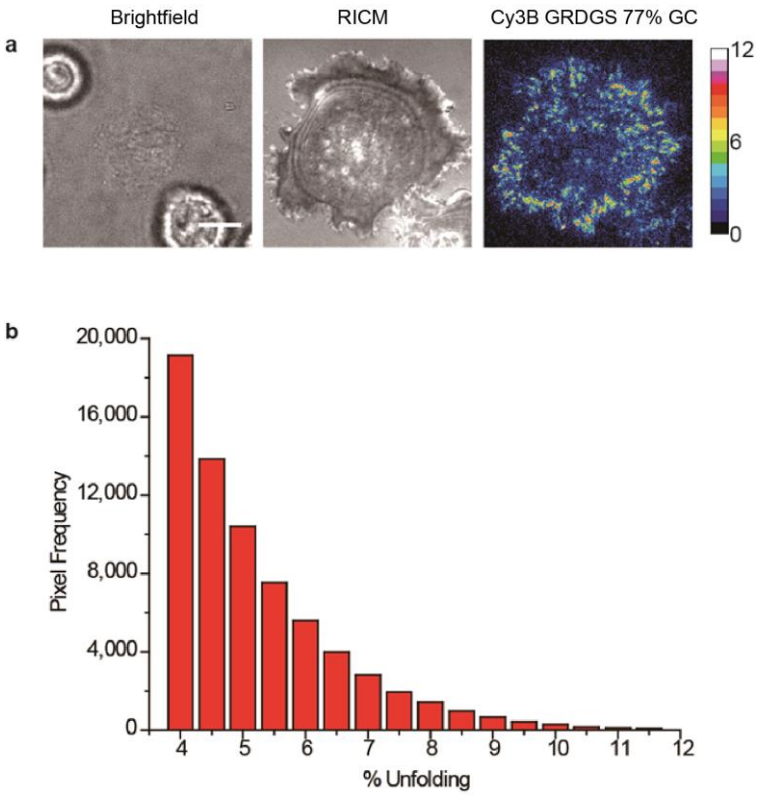

Supplementary Figure 11. Integrin mechanical response on 77% GC tension probe surface exclusively displaying the linear GRGDS peptide. (**a**) Representative brightfield, RICM and % unfolded map of a cell cultured on the 77% GC tension probe surface for 20 min. Scale bar: 10 μm. (**b**) Histogram showing the frequency of pixels displaying different levels of % unfolding. Data were collected and analyzed from 6 cells. Note that a significant number of the 77% GC probes with GRGDS peptide were unfolded (with % unfolding values ranging from 4-12%) on these surfaces. In contrast, % unfolding values were diminished and ranged from 0-4% when the GRGDS peptide was presented in a binary mixture with cRGD peptides (Fig. 4b), thus showing that integrins display chemo-mechanical specificity.

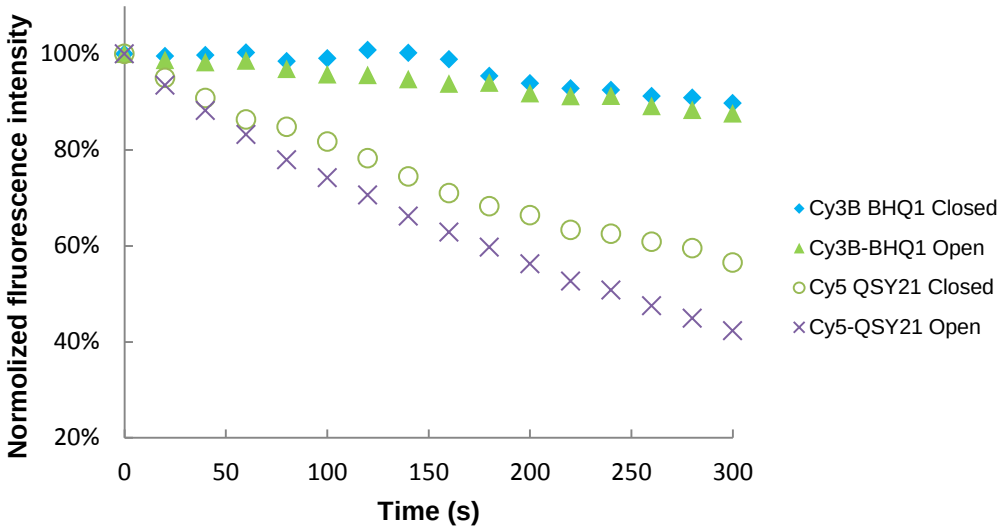

Supplementary Figure 12. Photostability of Cy5-QSY 21 and Cy3B-BHQ1 reporter pairs. Plot shows the fluorescence intensity of MTFM sensors that are in the fully opened or closed conformation. Images were acquired every 20 s using 400 ms exposure time in PBS. Plot indicates better Cy3B photostability in comparison to Cy5.

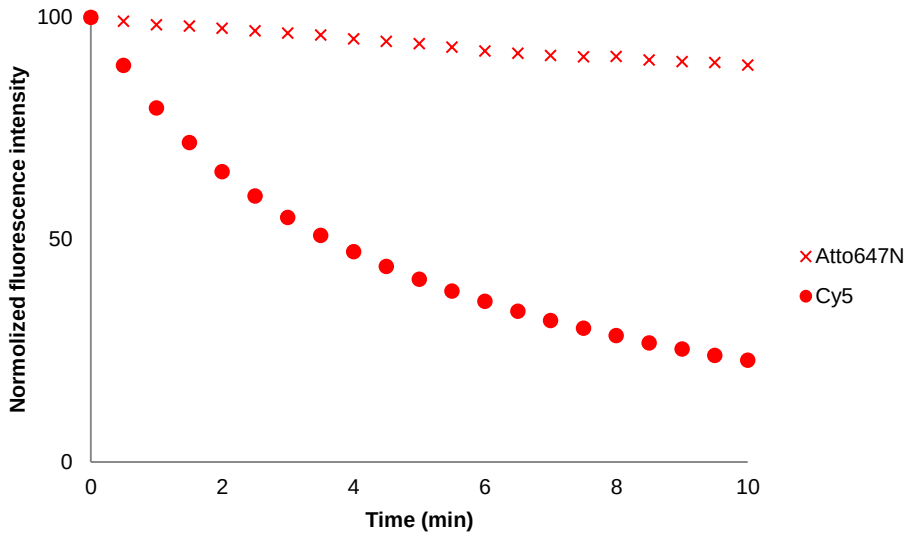

Supplementary Figure 13. Photostability of Cy5 and Atto647N. Plot shows the normalized fluorescence intensity of the Cy5 and Atto647N modified glass slides using a 1 s epifluorescence exposure time. Under these conditions (1 X PBS, RT), Atto647N was much more photostable.

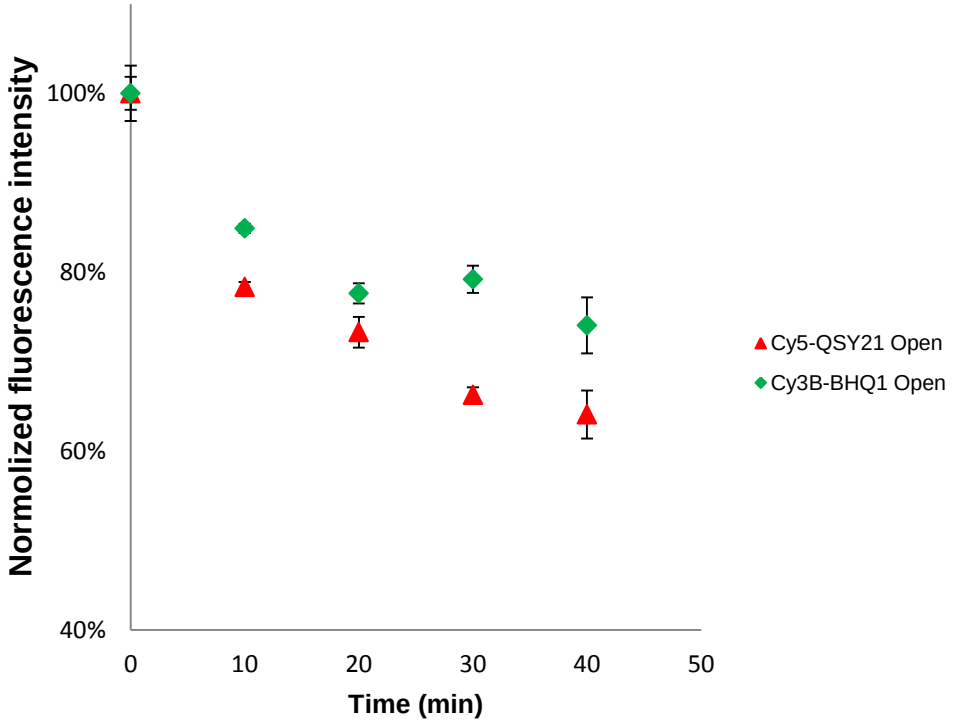

Supplementary Figure 14. Chemical stability of MTFM DNA-based sensors. Plot showing the fluorescence intensity of unfolded sensors (45 mer) for two different fluorophore-quencher pairs. The images were acquired every 10 min, with 400 ms exposure time for Cy3B and 1s exposure time for Cy5. Note that these imaging parameters were identical to the ones used for the cell experiment with multiplexed tension probes. Cy3B demonstrated better chemical stability compared to Cy5 tagged tension probes. To better simulate the cell experiments, we recorded fluorophore stability using cell media (including serum) and also adding cells to the chamber. Cells failed to attach since these sensors lacked the RGD peptide.

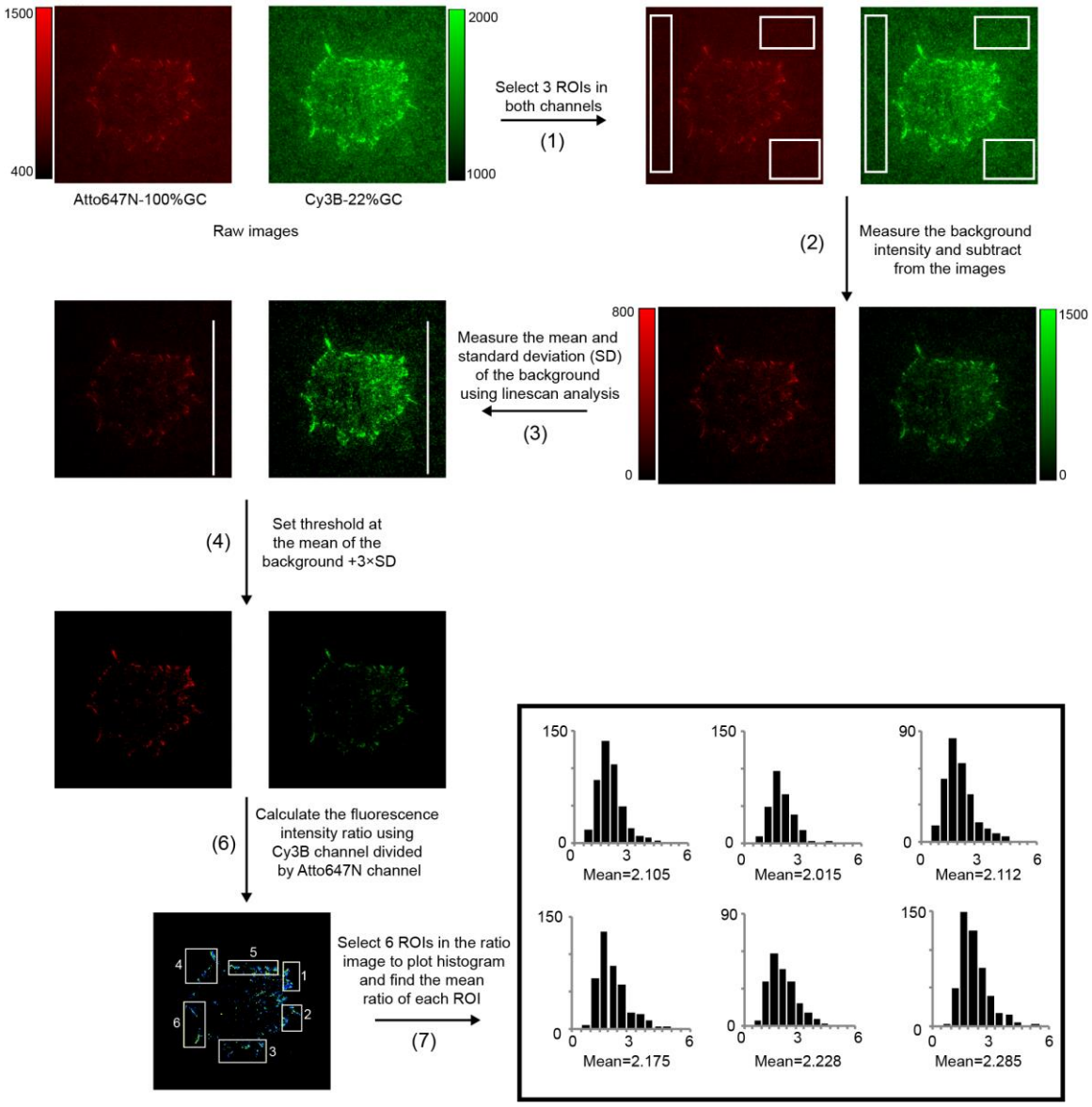

Supplementary Figure 15. Flowchart describing the analysis used to compare the ratio of the signal intensities from the multiplexed probes. See main text Fig. 5d.

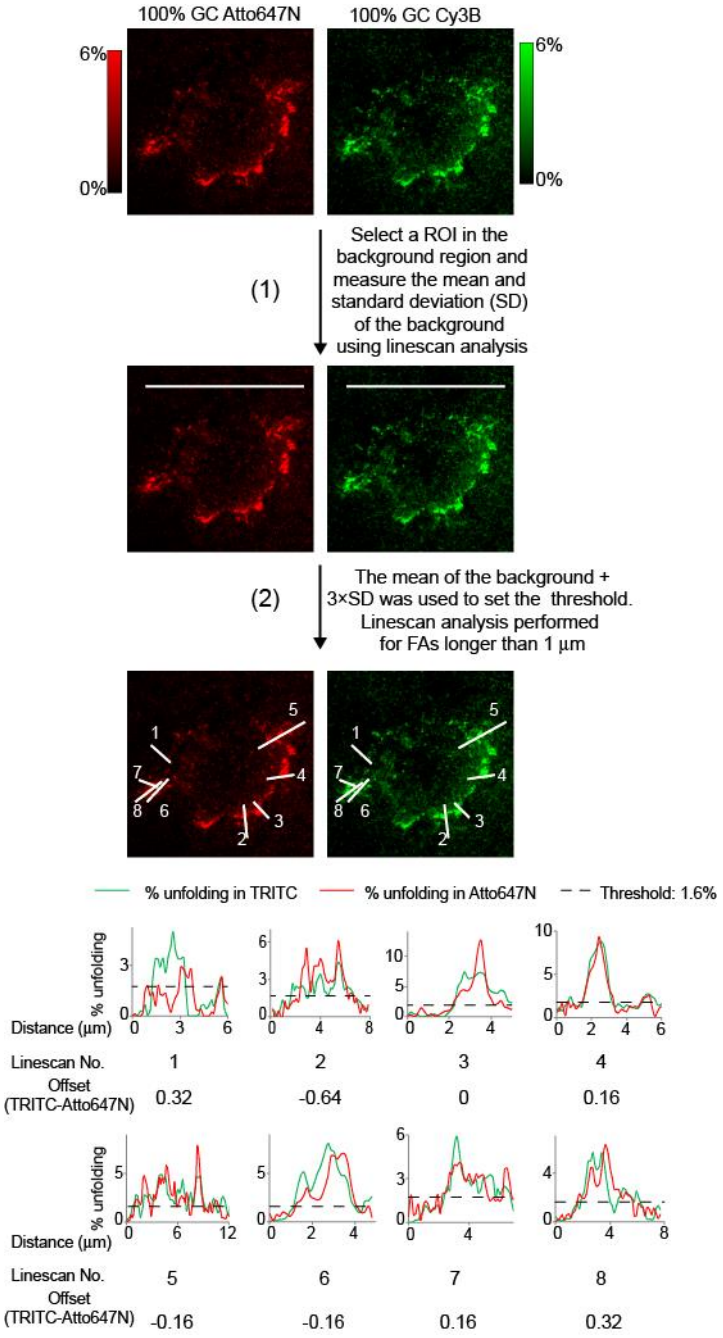

Supplementary Figure 16. Flowchart describing the analysis used to compare the offset of the starting position of the FAs in the two fluorescence channels. This analysis was used to generate the histogram shown in main text Fig. 5e. For the multiplexed probe data set, we subtracted the start position of the tension signal obtained from the 22% GC probe from that of the tension signal in the 100% GC probe channel.

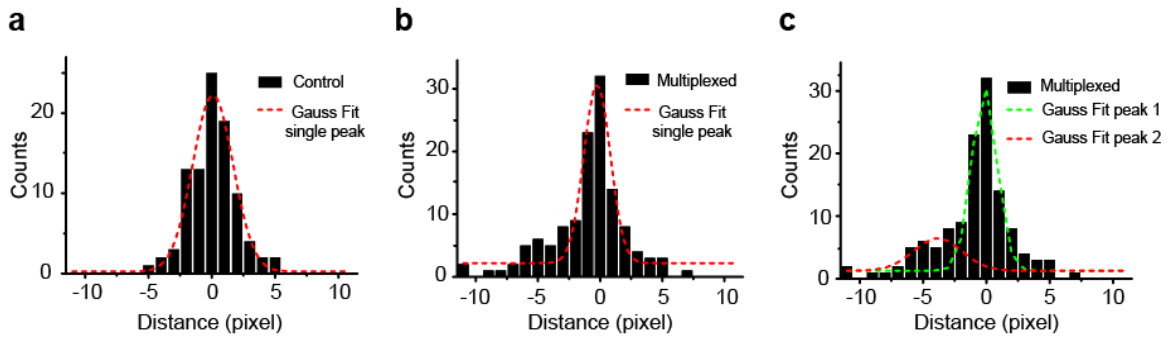

	Control Single Peak Fit		Multiplexed Single Peak Fit		Multiplexed Two Peak Fit			
	Value	Standard Error	Value	Standard Error	Value	Standard Error	Value	Standard Error
y0	0.3	0.4	2.2	0.6	1.3	0.5		
xc	0.1	0.1	-0.24	0.09	-0.2	0.1	-3.8	1.0
w	3.2	0.2	2.1	0.2	2.0	0.2	3.7	2.0
A	88.0	5.8	76.1	6.6	72.6	10.1	24.7	12.5
Reduced Chi-sqr	2.5		5.8		3.3			
Adj.R-Square	0.95		0.90		0.96			

Supplementary Figure 17. Fitting the offset in the start position of tension between the two multiplexed probes. The offset data from control and multiplexed probes was plotted in histograms (Fig. 5e). (**a**) Red dashed line represents the single peak Gaussian fit of the control experiment histogram, where both probes were encoded using 100% GC hairpins. The fit was performed using OriginPro 8.5 data analysis package and the parameters of the fit are shown in the table below. The adjusted R^2 value was 0.95 and the reduced χ^2 value was 2.5, indicating a valid fit to the data. (**b**) Red dashed line represents the single peak Gaussian fit of the multiplexed data. The adjusted R^2 value was 0.90 and the reduced χ^2 value was 5.8 indicating a poor fit for the data when compared to (**a**). To confirm the control and multiplexed histograms represent different distributions, we performed a comparison of the two data sets (F-test) in Origin and found that the two sets are statistically different ($p=0.038$, which is <0.05). (**c**) To better fit the multiplex histogram, we used two Gaussian functions, which were software generated and are shown in the dashed red and green lines. The center of the red peak was -0.2 $\pm$ 0.1 pixels, which is similar to the control center position of 0.1 $\pm$ 0.1 pixels. This indicates no difference in the start position of tension in the two the channels. The green peak center position was -3.8 $\pm$1 pixels, indicating that there was a subset of tension signals that displayed the 100% GC probe closer to the cell edge by ~0.5 microns. Based on the adjusted R^2 value (0.96 versus 0.90) and the reduced χ^2 (3.3 versus 5.8), the multiplexed data was more accurately fit to two Gaussian distributions, thus confirming that the two data sets represent distinct populations. 1 pixel= 160 nm.

Supplementary Table 1. Oligonucleotide sequences.

ID	DNA Sequence
Anchor strand	5’-/5AmMC6/-CGC ATC TGT GCG GTA TTT CAC TTT –/3BioTEG/-3’
Anchor strand with BHQ-1*	5’-/BHQ 1/-CGC ATC TGT GCG GTA TTT CAC TTT-/ Biotin/-3’
Ligand strand	5’-/5Hexynyl/-TTT GCT GGG CTA CGT GGC GCT CTT–/3AmMO/-3’
22% GC	5'-GTG AAA TAC CGC ACA GAT GCG TTT- GTA TAA ATG TTT TTT TCA TTT ATA C -TTT AAG AGC GCC ACG TAG CCC AGC -3’
77% GC	5'-GTG AAA TAC CGC ACA GAT GCG TTT- GTA CGC GCG TTT TTT TCG CGC GTA C-TTT AAG AGC GCC ACG TAG CCC AGC -3’
Complementary sequence to 77% GC hairpin	5'- AAA GTA CGC GCG AAA AAA ACG CGC GTA CAAA -3'
100% GC	5'-GTG AAA TAC CGC ACA GAT GCG TTT- GCG CGC GCG CGC TTT TGC GCG CGC GCG C-TTT AAG AGC GCC ACG TAG CCC AGC -3’
Complementary sequence to 100% GC hairpin	5’-AAA GCG CGC GCG CGC AAA AGC GCG CGC GCG CAA A-3’
H45	5’-GTG AAA TAC CGC ACA GAT GCG TTT- CGA TAA CTT TTT TTT TTT TTT TTT TTT TTG TTA TCG –TTT AAG AGC GCC ACG TAG CCC AGC -3’
Complementary sequence to H45	5’- AAA CGA TAA CAA AAA AAA AAA AAA AAA AAA AAA AAG TTA TCG AAA-3’

*Anchor strand with BHQ-1 was purchased from Biosearch Technology (Novato, CA). Underlined sequences represent regions that are expected to fold into hairpin structures.

Supplementary Table 2. MALDI-TOF analysis. The table below summarizes the calculated and observed molecular weights (MW) of all synthesized intermediates and final ligand and anchor strands products used in the current work.

Product	MW (calc.)	MW (obs)
c(RGDfK(PEG-PEG))-azide	977.1	970.6
Gly-Arg-Gly-Asp-Ser-azide	573.6	574.2
c(RGDfK(PEG-PEG))-ligand strand	8706.1	8714.2
Gly-Arg-Gly-Asp-Ser-ligand strand	8302.6	8314.1
c(RGDfK(PEG-PEG))-ligand strand-Cy5	9207.3	9203.2
Gly-Arg-Gly-Asp-Ser-ligand strand-Cy5	8803.8	8805.1
c(RGDfK(PEG-PEG))-ligand strand-Atto647N	9434.6	9452.6
c(RGDfK(PEG-PEG))-ligand strand-Cy3B	9357.1	9372.4
Gly-Arg-Gly-Asp-Ser-ligand strand-Cy3B	8953.6	8971.4
QSY 21 labeled anchor strand	8749.8	8747.4

Supplementary Table 3. Caculated $F_{1/2}$ for 22% GC, 77% GC and 100% GC tension probes at experimental conditions (37 °C, 140.5 mM Na^+ and 0.4 mM Mg^{2+}).

ID	Length mer	Sequence	ΔG_{IDT} kJ/mol	$\Delta G_{stretch}$ kJ/mol	ΔG kJ/mol	Δx nm	$F_{1/2}$ pN
22% GC	25	GTA TAA ATG TTT TTT TCA TTT ATA C	12.4	9.5	21.9	8.6	4.2
77% GC	25	GTA CGC GCG TTT TTT TCG CGC GTA C	40.2	9.5	49.6	8.6	9.6
100% GC	28	GCG CGC GCG CGC TTT TGC GCG CGC GCG C	84.4	10.7	95.2	9.9	16.0

Supplementary Table 4. Quenching efficiency for different fluorophore-quencher pairs. Cy3B-BHQ 1, Atto647N-QSY and Cy5-QSY 21 demonstrated the highest QE among these measured pairs.

	BHQ-1 QE%	QSY 21 QE%
Atto647N		94.2% ± 0.2%
Cy5		94.9% ± 0.1%
Cy3B	95.0% ± 0.3%	90.6% ± 0.2%
TAMRA	64.9% ± 3.6%	86.4% ± 0.4%
Alexa Fluor® 488	74.2% ± 1.3%	
Fluorescein	62.6% ± 3.6%	

Supplementary Table 5. Single color Cy3B imaging parameters

Reporter dye	Cy3B	Cy3B
Hairpin sensor	77%GC, 22%GC	100%GC
Exposure time	400ms	400ms
QE	94.3%	95.0%
Conversion of $\frac{I_{DA}}{I_D}$ (*x*) to % unfolded(*y*)	*y* = (1.059*x* - 0.059)*100	y = (1.053*x* - 0.053)*100

Supplementary Table 6. Dual color Cy3B-100%GC and Cy5- 77%GC, 22%GC imaging parameters.

Reporter dye	Cy3B	Cy5
Hairpin sensor	100%GC	77%GC, 22%GC
Exposure time	400ms	900ms
QE%	92.3%	95.7%
Conversion of $\frac{I_{DA}}{I_D}$ (*x*) to % unfolded (*y*)	*y* = (1.083*x* - 0.083)*100	*y* = (1.044*x* - 0.044)*100
Bleed through	7.9%	Negligible

Supplementary Table 7. Dual color Cy3B-77%GC, 22%GC and Cy5-100% imaging parameters.

Reporter dye	Cy3B	Cy5
Hairpin sensor	77%GC, 22%GC	100% GC
Exposure time	400ms	900ms
QE%	94.3%	96.6%
Conversion of $\frac{I_{DA}}{I_D}$ (*x*) to % unfolded(*y*)	*y* = (1.059*x* - 0.059)*100	*y* = (1.035*x* - 0.035)*100
Bleed through	3.6%	Negligible

Supplementary Table 8. Dual color Cy3B-22%GC and Atto647N-100%GC imaging parameters.

Reporter dye	Cy3B	Cy5
Hairpin sensor	22%GC	100%GC
Exposure time	500ms	1s
QE%	92.2%	94.2%
Conversion of $\frac{I_{DA}}{I_D}$ (*x*)	*y* = (1.084x - 0.084)*100	*y* = (1.061x - 0.061)*100

to % unfolded(*y*)		
Bleed through	2.1%	Negligible

Supplementary Table 9. Dual color Cy3B-100%GC and Cy5-22%GC imaging parameters.

Reporter dye	Cy3B	Cy5
Hairpin sensor	100%GC	22%GC
Exposure time	500ms	1s
QE%	92.1%	94.0%
Conversion of $\frac{I_{DA}}{I_D}$ (*x*) to % unfolded(*y*)	*y* = (1.086x - 0.086)*100	*y* = (1.063x - 0.063)*100
Bleed through	3.6%	Negligible

Supplementary Note 1

Synthesis of the c(RGDfK(PEG-PEG)) ligand strand with Cy5/Cy3B/Atto647N (Cy5 shown as an example)

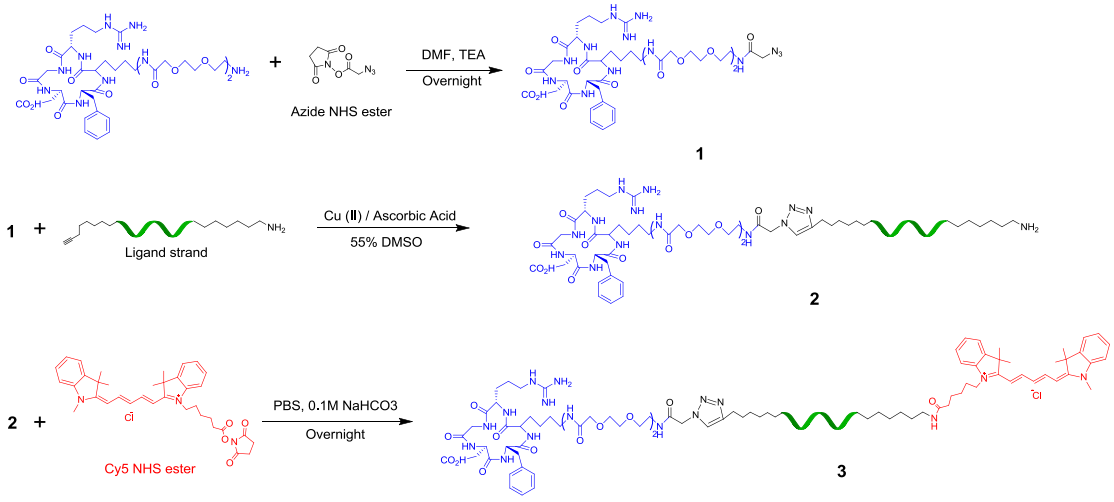

The fluorescently labeled cyclic-peptide-oligonucleotide conjugate was generated in a three-step procedure. In the first step, the primary amine of the c(RGDfK(PEG-PEG)) peptide was activated with an azide group by coupling 100 nmoles of the peptide with 150 nmoles of azide-NHS linker in 10 µL of DMF. To this reaction mixture, 0.1 µL of neat triethylamine was added as an organic base, and the reaction was allowed to proceed for 12 h. The product, **1**, of this reaction was purified by reverse phase HPLC (Supplementary Fig. 2a) (flow rate 1 mL/min; solvent A: 0.1 M TEAA, solvent B: 100% acetonitrile; initial condition was 10% B with a gradient of 0.5% per min). The yield of the reaction was determined to be 99% by integrating the HPLC peaks. MALDI-TOF MS was then used to confirm the mass of the product (Supplementary Table 2).

In the following step, the peptide was coupled to the oligonucleotide using a 1,3-dipolar cycloaddition “click” reaction and following the manufacturer’s protocols listed on the Lumiprobe corporation website. Briefly, 20 µL reaction buffer containing 500 mM alkyne-modified ligand strand, 750 mM product **1**, 0.5 mM ascorbic acid, 0.5 mM Cu-TBTA (Tris[(1-benzyl-1H-1,2,3-triazol-4-yl)methyl]amine) complex and 50% DMSO. This reaction was allowed to proceed for 12 h. After purification using a P4 gel, the product, **2**, was separated from unlabeled oligonucleotides by HPLC (Supplementary Fig. 2b) (flow rate 1 mL/min; solvent A: 0.1M TEAA, solvent B: 100% acetonitrile; initial condition was 10% B with a gradient of 1% per min), and confirmed by MALDI-TOF MS (Supplementary Table 2).

In the final step, the fluorescent dye, Cy5-NHS or Cy3B-NHS, was coupled to the 3’ amine group of DNA-peptide conjugate, **2,** by adding 1 µL of 1 mM DNA and 1 µL of 1 M sodium bicarbonate to 7 µL of PBS. Then, 1 µL of 10 mM dye-NHS ester (10-fold molar excess) was

added to the DNA mixture. The reaction was allowed to incubate at room temperature overnight. After P4 gel purification, the product, **3**, was separated from **2** by HPLC while monitoring channels at 260/640 nm or 260/560 nm (Supplementary Fig. 2c) (flow rate 1 mL/min; solvent A: 0.1M TEAA, solvent B: 100% acetonitrile; initial condition was 10% B with a gradient of 1% per min). The final product was verified by MALDI-TOF MS (Supplementary Table 2).

Synthesis of the Gly-Arg-Gly-Asp-Ser ligand strand with Cy5/Cy3B/Atto647N. The linear peptide-oligonucleotide conjugate was generated using a similar procedure to that used for the cyclic peptide coupling (*vide supra*). HPLC and MALDI-TOF were used to verify the final product (Supplementary Table 2).

Synthesis of the QSY 21 labeled anchor oligonucleotide strand. The quencher-oligonucleotide conjugate was generated using a similar procedure to that used for generating the Cy5/Cy3B coupled oligonucleotides. HPLC and MALDI-TOF were used to verify the final product (Supplementary Table 2).

Supplementary Note 2

To verify that our calculations and assumptions are in agreement with prior work, we calculated the free energy of unfolding a library of 20 hairpin sequences that were published in Woodside et al.'s work[3] and benchmarked the results in the following table. We found that the results were in general agreement. Subsets of this library of hairpins highlighting the role of stem length and GC content are plotted in the following figure, thus illustrating the agreement for sequences that are equal to, or less than 25 bases long. Accordingly, we used tension sensor hairpins with total length of approximately 25 nucleotides and stem lengths shorter than 12 base pairs, to ensure the accuracy of $F_{1/2}$.

Hairpin		**Literature Data (obtained from Woodside et al.)**			**Calculated Data**		
Hairpin name	mer	Δx Nm	$F_{1/2}$ pN	ΔG, kJ/mol	ΔG_{IDT} kJ/mol	$\Delta G_{stretch}$ kJ/mol	ΔG,calc. kJ/mol
6R50/T4	16	5.1 ± 0.3	8.0 ± 0.7	**25 ± 3**	20.9	5.6	**26.5**
8R50/T4	20	7.2 ± 0.3	8.4 ± 0.6	**38 ± 3**	31.5	7.3	**38.8**
10R50/T4	24	8.7 ± 0.3	10.5 ± 0.6	**54 ± 4**	43.4	9.0	**52.4**
15R53/T4	34	13.6 ± 0.3	12.3 ± 0.4	**100 ± 6**	76.5	13.3	**89.8**
20R50/T4	44	17.8 ± 0.3	13.6 ± 0.4	**146 ± 8**	108.8	17.6	**126.5**
25R52/T4	54	20.9 ± 0.5	14.5 ± 0.7	**183 ± 10**	146.8	22.0	**168.8**
30R50/T4	64	26.5 ± 0.5	14.4 ± 0.7	**227 ± 11**	174.3	26.3	**200.6**
15R60/T3	33	13.0 ± 0.5	10.8 ± 0.8	**91 ± 9**	76.0	12.9	**88.9**
15R60/T4	34	13.5 ± 0.3	13.3 ± 0.5	**108 ± 6**	82.9	13.3	**96.2**
15R60/T6	36	14.8 ± 0.3	11.3 ± 0.7	**100 ± 6**	82.9	14.2	**97.0**
15R60/T8	38	15.2 ± 0.5	10.3 ± 0.5	**95 ± 7**	77.5	15.1	**92.6**
15R60/T12	42	17.3 ± 0.5	9.7 ± 0.5	**98 ± 7**	76.7	16.8	**93.5**
15R60/T15	45	18.6 ± 0.6	9.1 ± 0.8	**98 ± 10**	76.0	18.1	**94.0**
15R60/T20	50	20.8 ± 0.7	8.1 ± 0.9	**90 ± 12**	74.4	20.2	**94.6**
15R60/T30	60	25.7 ± 1	7 ± 1	**96 ± 25**	70.1	24.6	**94.6**
20R0/T4	44	17.6 ± 0.3	7.9 ± 0.4	**86 ± 5**	63.6	17.6	**81.2**
20R25/T4	44	17.6 ± 0.4	10.6 ± 0.5	**112 ± 8**	86.9	17.6	**104.5**
20R55/T4	44	18.1 ± 0.3	13.8 ± 0.4	**146 ± 7**	115.2	17.6	**132.9**
20R75/T4	44	19.3 ± 0.4	15.2 ± 0.5	**175 ± 10**	135.7	17.6	**153.4**
20R100/T4	44	19.0 ± 0.4	19.3 ± 0.8	**220 ± 13**	171.4	17.6	**189.1**

Experimental Conditions: 200 mM monovalent salt and 25 °C.

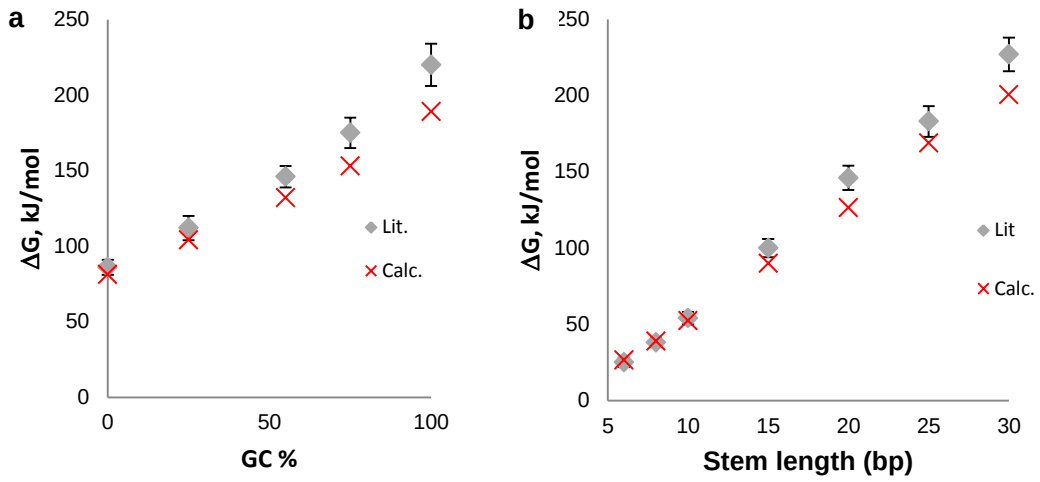

Comparisons of calculated total free energy associated with hairpin unfolding using $\Delta G = \Delta G_{IDT} + \Delta G_{stretch}$ with the published data from Woodside et al. Plots showing the total change in free energy of unfolding a hairpin as a function of GC content (**a**), and stem length (**b**). Gray diamonds represent the values obtained from Woodside et al., while the red x indicates calculated free energy values in this work.